Resonant cavitylike modes in dielectric photonic crystals made of collections of subwavelength cylinders

Ruey-Lin Chern[1,*] and Didier Felbacq[2]
[1]*Institute of Applied Mechanics, National Taiwan University, Taipei 106, Taiwan, Republic of China*
[2]*GES UMR-CNRS 5650, Université de Montpellier II, Bâtiment 21, CC074, Place E. Bataillon, 34095 Montpellier Cedex 05, France*
(Received 9 June 2009; revised manuscript received 30 September 2009; published 16 November 2009)

We investigate resonant cavitylike modes in dielectric photonic crystals made of collections of subwavelength cylinders with high permittivity. A large number of collective modes appear for TE polarization (where magnetic fields are oriented along the cylinder axis), which possess similar features of resonant cavity modes that occur in polaritonic structures. These modes are dispersionless in nature and intensively gathered around an asymptotic frequency that depends on the subwavelength cylinders. The typical resonant cavitylike modes are illustrated with the magnetic field distributions at the resonant frequencies. In particular, the field pattern in the building block shows a close resemblance to TE_{nm} mode of an isolated waveguide. The respective cutoff frequency at large oscillation orders serves as the asymptotic frequency of resonant cavitylike modes.

DOI: 10.1103/PhysRevB.80.205115 PACS number(s): 41.20.Jb, 42.70.Qs, 78.20.Bh

I. INTRODUCTION

Metamaterials are artificial structures which possess properties not available in naturally occurring materials.[1,2] The unusual properties come from the interaction of electromagnetic waves with the structure rather than directly from the material composition. To treat in effect the metamaterial as a homogeneous medium, the microstructures that compose the medium have to be much smaller than the wavelength. Major characteristics of a metamaterial are therefore quasistatic in nature.

A useful way to describe the metamaterial properties is through the use of effective parameters, such as the effective permittivity ε_{eff} and effective permeability μ_{eff}. The two quantities characterize the response of a medium to the electric and magnetic fields, respectively. For a metamaterial made of subwavelength microstructures, the overall effective properties may differ from any of the constituent materials. In particular, the effective parameters are valid in the quasistatic regime, where the frequency is relatively lower, but the retardation effect is still important. In this regime, the field distribution tends to be uniform at a large length scale. At a small length scale comparable with the microstructure size, the variation in fields may be significant.

Due to the resonance of fields inside the microstructures, metamaterials may exhibit counterintuitive properties such as a negative permeability.[1] In particular, a strong magnetic activity may arise in a photonic structure with large dielectric contrast.[3] The effective permeability μ_{eff} of the structure was shown to experience a Lorentz-type anomalous dispersion and this structure is regarded as a dielectric metamaterial.[4] Near a particular resonant frequency, μ_{eff} drastically changes from a very large positive value to a very large negative one. The magnetic response of the dielectric metamaterial thus resembles the electric response of a polar material. In this regard, certain features associated with polaritonic structures[5–9] may occur as well in a photonic structure made of such dielectric metamaterial.

One of the most distinguished features for polaritonic structures is the appearance of resonant cavity modes. These modes come from the strong coupling of photons with phonons in the polar material and are closely related to interesting properties such as flux expulsion and node switching.[5] As the frequency approaches the transverse-optical phonon frequency ω_T, the polar material becomes a very large-index medium. The electromagnetic fields are therefore trapped in the medium and the polaritonic structure behaves like a collection of cavities.

In this study, we investigate resonant cavitylike modes in a special realization of the photonic crystal, whose building block consists of a collection of subwavelength cylinders with high permittivity. In view of the effective permeability, the underlying photonic structure behaves like a *magnetic* analog of polaritonic crystal. The existence of resonant cavitylike modes is manifest on the dispersion characteristics in two aspects. First, a large number of collective modes appear and gather around an asymptotic frequency for TE polarization. The modes possess features similar to those of resonant cavity modes occurring in polaritonic structures. Second, the typical resonant modes exhibit a highly localized field distribution within the building block, outside which the field amplitudes are nearly zero. This is another distinguished feature of resonant cavity modes. In particular, the magnetic fields in the building block show a pattern analogous to that of TE_{nm} mode of an isolated waveguide. The respective cutoff frequency at large oscillation orders serves as the role of asymptotic frequency for resonant cavitylike modes.

II. BASIC EQUATIONS

A. Effective permeability model

Consider a periodic array of square cylinders with width s and dielectric constant ε_1, embedded in a background material with dielectric constant ε. The array period h is assumed to be much smaller than the wavelength λ in such a way that the dielectric structure can be regarded as a *homogeneous* medium. Let ε_1 be substantially larger than ε. A strong magnetic activity arises due to the presence of Mie resonance associated with the dielectric cylinders.[3] Near a resonance,

the polarization currents are circulating around each dielectric cylinder (about its axis) and tend to approach their maximum values. As a result, the magnetic fields are highly localized in the dielectric region. The effective permeability μ_{eff} of the dielectric structure becomes frequency dependent and exhibits an *anomalous* dispersion around the resonant frequency.

According to the theory of mesoscopic magnetism,[4,10,11] the effective permeability μ_{eff} is described by an explicit expression as

$$\mu_{\text{eff}}(\omega) = 1 - f \sum_{n,m=1,3,5,\ldots} \frac{\beta_{nm}\omega^2}{\omega^2 - \omega_{nm}^2}, \tag{1}$$

where $f=s^2/h^2$ is the filling fraction of cylinders. This formula manifests itself as a sum of Lorentz-type oscillators; each oscillator is characterized by a resonant frequency ω_{nm} and a weighting coefficient β_{nm} with respect to the oscillation orders n and m. In particular, ω_{nm} is identified as the waveguide mode frequency, which can be realized by the fact that the magnetic fields are largely confined in the high-dielectric region and the cylinder behaves like a waveguide or cavity resonator. The coefficient β_{nm} is a measure of the oscillator strength and determined by the eigenfield associated with the resonant frequency ω_{nm} as[12]

$$\beta_{nm} = \frac{\langle \psi_{nm}, 1\rangle^2}{\langle \psi_{nm}, \psi_{nm}\rangle\langle 1,1\rangle}, \tag{2}$$

where ω_{nm} and ψ_{nm} are the nmth solution pair of the eigensystem

$$-\nabla^2\psi = \varepsilon_1\left(\frac{\omega}{c}\right)^2\psi, \tag{3}$$

defined at the *interior* of high-dielectric region Ω with $\psi=0$ on its boundary, and the inner product $\langle f,g\rangle \equiv \int_\Omega f^* g d\tau$ is an integral taken over the region Ω. For simple geometries such as square or circular cylinders, both ω_{nm} and β_{nm} can be analytically obtained.[13] In the present problem, the cylinder is of square shape and the solutions are given as

$$\omega_{nm} = \frac{\pi c\sqrt{n^2+m^2}}{s\sqrt{\varepsilon_1}}, \tag{4}$$

$$\psi_{nm} = \cos\left(\frac{n\pi x}{s}\right)\cos\left(\frac{m\pi y}{s}\right), \tag{5}$$

$$\beta_{nm} = \frac{64}{n^2m^2\pi^4}. \tag{6}$$

Note that ω_{nm} and ψ_{nm} correspond to the resonant frequency and mode pattern, respectively, of TE_{nm} mode for a square waveguide.[14]

Near the lowest-order resonance ($n=m=1$), Eq. (1) is approximated as

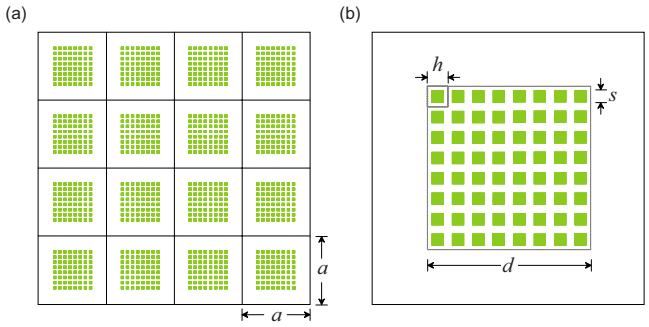

FIG. 1. (Color online) Schematics of (a) the photonic crystal made of collections of subwavelength cylinders and (b) the building block in the unit cell.

$$\mu_{\text{eff}}(\omega) = 1 - \frac{f\beta_{11}\omega^2}{\omega^2 - \omega_{11}^2}, \tag{7}$$

where $\beta_{11}=64/\pi^4\approx 0.657$ and $\omega_{11}=\pi c\sqrt{2}/s\sqrt{\varepsilon_1}$. This permeability model is also applicable to the magnetic response of split-ring resonators,[12] where the resonance factor $\beta_{11}\approx 1$. In analogy with the dielectric model of polar materials, Eq. (7) can be rewritten as

$$\mu_{\text{eff}}(\omega) = \mu_\infty\left(\frac{\omega^2-\omega_{mL}^2}{\omega^2-\omega_{mT}^2}\right), \tag{8}$$

where $\mu_\infty = 1 - f\beta_{11}$ is the permeability at high frequency, $\omega_{mT}=\omega_{11}$ and $\omega_{mL}=\omega_{mT}/\sqrt{\mu_\infty}$ are regarded as the *magnetic* analogs of transverse- and longitudinal-optical-phonon frequencies, respectively.[15]

B. Photonic crystal of subwavelength cylinders

Now consider a photonic crystal made of the aforementioned subwavelength cylinders. The building block is a square column of width d, consisting of a collection of dielectric cylinders at the subwavelength scale. The schematics of the photonic crystal and the building block in the unit cell are shown in Fig. 1. In this configuration, the subwavelength cylinders are responsible for the existence of resonant cavitylike modes in a nonpolaritonic structure. Basic features of resonant cavitylike modes are either manifest or implied in the dispersion characteristics. For propagation of waves parallel to the lattice plane, the time-harmonic magnetic mode (with time dependence $e^{-i\omega t}$) is described by

$$-\nabla\cdot\left(\frac{1}{\varepsilon}\nabla H\right) = \left(\frac{\omega}{c}\right)^2 H. \tag{9}$$

It is sufficient to solve the underlying problem (periodic structure of infinite extent) in one unit cell along with the Bloch condition

$$H(\mathbf{r}+\mathbf{a}_i) = e^{i\mathbf{k}\cdot\mathbf{a}_i}H(\mathbf{r}) \tag{10}$$

applying at the unit-cell boundary, where $\mathbf{k}$ is the Bloch wave vector and $\mathbf{a}_i (i=1,2)$ is the lattice translation vector.

In the present problem, the unit cell of the photonic crystal contains a collection of subwavelength cylinders. Compared to usual photonic structures, where only one or few

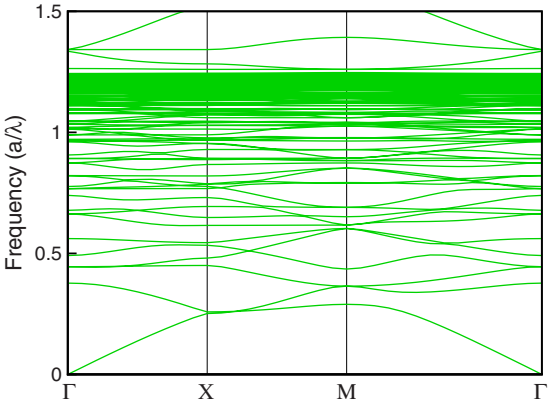

FIG. 2. (Color online) Dispersion diagram for the photonic crystal made of collections of subwavelength cylinders, where $\varepsilon_1 = 200+5i$, $\varepsilon=1$, $d/a=0.8$, $h/a=0.05$, and $s/h=0.8$.

elements are present in each unit cell, the building block of the underlying structure presents itself a more delicate (or complex) geometry with substructures (the cylinders) much smaller than the unit cell size. Accordingly, the eigenfields may exhibit variations at the corresponding (smaller) length scale and a higher precision scheme is required to resolve the underlying problem.

For a photonic crystal with complex geometry, the dispersion relations can be efficiently solved by the inverse iteration method.[16–18] In this approach, the eigensystem, Eq. (9), is solved by making good use of the *Hermitian* property of the differential operator. The important step is the calculation of the Rayleigh quotient

$$R_Q = \frac{\langle \mathbf{x}, \mathbf{A}\mathbf{x} \rangle}{\langle \mathbf{x}, \mathbf{x} \rangle}, \tag{11}$$

where $\mathbf{A}$ is the matrix constructed by discretization of the differential operator, $\mathbf{x}$ is the vector consisting of all discrete values of H (over the unit cell), and the inner product $\langle \cdot, \cdot \rangle$ is taken over the unit cell. An initial guess of $\mathbf{x}$, usually prescribed as a random distribution, is used to give a first value of R_Q, which in turn is utilized to refine the vector $\mathbf{x}$ through solving a matrix inversion

$$(\mathbf{A} - \mu \mathbf{I})\mathbf{x}_n = \mathbf{x}_o, \tag{12}$$

where $\mathbf{x}_o$ and $\mathbf{x}_n$ are referred to as old and new values of $\mathbf{x}$, respectively, and μ is a parameter. This procedure is repeated until the Rayleigh quotient R_Q converges within a certain accuracy; the quotient R_Q and the vector $\mathbf{x}$ are then given as the solution pair of the eigenvalue and eigenfunction. More details of this approach can be found in Refs. 16 and 17.

III. RESULTS AND DISCUSSION

A. Collective frequency branches

Figure 2 shows the dispersion diagram for a photonic crystal made of collections of subwavelength cylinders, where $\varepsilon_1 = 200+5i$, $\varepsilon=1$, $d/a=0.8$, $h/a=0.05$, and $s/h=0.8$. A large number of frequency branches appear for TE polarization. As the frequency gets closer to $a/\lambda \approx 1.24$, more branches are observed. These collective modes have similar features to those of resonant cavity modes that occur in polaritonic structures.[6,8,9] They are dispersionless in nature; that is, their frequencies are insensitive to the change of wave vector. As a result, the corresponding frequency branches tend to be flattened. In a polaritonic structure, the dispersionless nature comes from the strong coupling of photons with phonons in the polar material.[8] As the underlying photonic crystal is made of a dielectric material, there is no such coupling behavior.

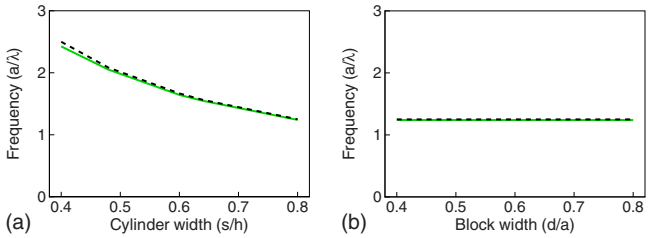

FIG. 3. (Color online) Variations in the asymptotic frequency for resonant cavitylike modes with respect to (a) cylinder width s, where $h/a=0.05$ and $d/a=0.8$, (b) block width d, where $h/a=0.05$ and $s/h=0.8$. The dashed line denotes the frequency ω_{mT}.

In the present problem, the dispersionless nature comes from the interaction of waves with the subwavelength structure. As indicated by Eq. (8), the effective permeability μ_{eff} reaches very large values when the frequency approaches $\omega_{mT} = \pi c\sqrt{2}/s\sqrt{\varepsilon_1} = 1.25(2\pi c/a)$ from below. In this situation, the subwavelength cylinders serve as a device for trapping electromagnetic fields and the building block acts like a high-index cavity. In a polaritonic structure, the asymptotic frequency of resonant cavity modes (that is, ω_T) is a property of the underlying material. For the photonic structure under study, the asymptotic frequency of resonant cavitylike modes depends on the subwavelength cylinders. Figure 3 shows the variations in the asymptotic frequency with respect to the cylinder width and block width. It is shown in Fig. 3(a) that the asymptotic frequency decreases as the cylinder width increases. In particular, this frequency is inversely proportional to the cylinder width and very close to ω_{mT} (denoted by the dashed line). On the other hand, the asymptotic frequency remains unchanged as the block width alters, as shown in Fig. 3(b).

B. Localized field patterns

The features of resonant cavitylike modes are further illustrated with the resonant field patterns. Figure 4 shows the magnetic field contours of four typical resonant modes at $a/\lambda \approx 0.561$, 0.964, 1.201, and 1.24 for the same photonic crystal in Fig. 2. Note that the fields are strongly localized in the collection of subwavelength cylinders, outside which the fields are nearly zero. In particular, the field patterns in the building block depict the resonant modes for a square waveguide as[14]

$$H_z(x,y) = \sin\left(\frac{p\pi x}{d}\right)\sin\left(\frac{q\pi y}{d}\right). \tag{13}$$

The patterns in Figs. 4(a)–4(d) correspond to $p,q=2$, 4, 8, and 16, respectively. As the orders (p,q) increase, the respec-

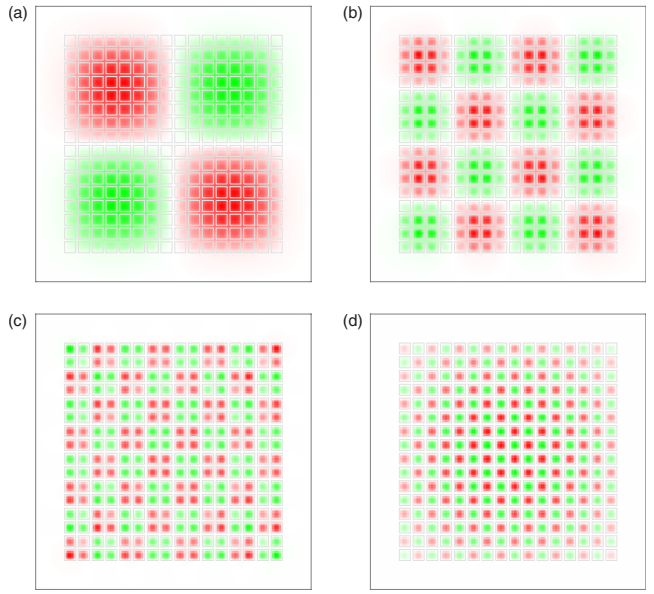

FIG. 4. (Color online) Magnetic field contours of four typical resonant cavitylike modes at (a) $a/\lambda \approx 0.561$, (b) $a/\lambda \approx 0.964$, (c) $a/\lambda \approx 1.201$, and (d) $a/\lambda \approx 1.24$ for the same photonic crystal in Fig. 2. The red and green colors denote the positive and negative values, respectively.

tive resonant frequency approaches an asymptotic value. This feature can be characterized by the dispersion relation of square waveguides filled with the effective medium as[6]

$$\omega = \frac{\pi c \sqrt{p^2 + q^2}}{d\sqrt{\varepsilon_{\text{eff}}\mu_{\text{eff}}(\omega)}}, \tag{14}$$

where the effective permittivity ε_{eff} is determined by using an approximate polarizability model for square cylinders[19] in the effective medium model as (see the Appendix for detail)

$$\varepsilon_{\text{eff}} \approx \varepsilon \frac{(1+1.29f)\varepsilon_1 + 1.29(1-f)\varepsilon}{(1-f)\varepsilon_1 + (1.29+f)\varepsilon}, \tag{15}$$

and $\mu_{\text{eff}}(\omega)$ is given by Eq. (8). The eigenfrequency $\hat{\omega}_{pq}$ associated with the orders (p,q) in Eq. (14) can be solved to give[8]

$$\hat{\omega}_{pq}^2 = \frac{2\Omega_{pq}^2\omega_{mT}^2}{\omega_{mL}^2 + \Omega_{pq}^2 + \sqrt{(\omega_{mL}^2 + \Omega_{pq}^2)^2 - 4\Omega_{pq}^2\omega_{mT}^2}}, \tag{16}$$

where $\Omega_{pq} = \pi c\sqrt{p^2+q^2}/d\sqrt{\varepsilon_{\text{eff}}\mu_\infty}$. It is shown in Eq. (16) that $\hat{\omega}_{pq} \to \omega_{mT}$ as $p,q \to \infty$. For the present configuration, $f=0.64$, $\varepsilon_{\text{eff}} \approx 4.95$, $\mu_\infty \approx 0.58$, and $\omega_{mL} \approx 1.64(2\pi c/a)$. It follows that $\hat{\omega}_{pq} \approx 0.722$, 1.074, 1.208, and $1.24(2\pi c/a)$ for $p,q=2$, 4, 8, and 16, respectively. The basic trend agrees with the resonant frequencies of the four typical resonant cavitylike modes (cf. Fig. 4). For larger (p,q), $\hat{\omega}_{pq}$ gives a better correspondence with the resonant modes.

In addition to the resonant cavitylike modes in Fig. 4, a number of modes with a very different characteristic appear in the *magnetic* polariton gap: $\omega_{mT} < \omega < \omega_{mL}$, where $\mu_{\text{eff}} < 0$. Figure 5 shows two typical resonant modes at $a/\lambda \approx 1.264$ and 1.335. In contrast with resonant cavitylike

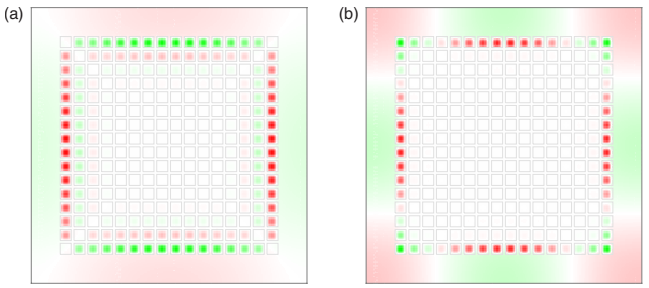

FIG. 5. (Color online) Magnetic field contours of two typical defectlike modes at (a) $a/\lambda \approx 1.264$ and (b) $a/\lambda \approx 1.335$ for the same photonic crystal in Fig. 2.

modes, the fields in Fig. 5 are distributed in the background material and nearly zero in the interior of the building block. This is a special feature of defectlike states that occur in a polaritonic crystal.[6] When the frequency is near ω_{mL} (where $\mu_{\text{eff}} \approx 0$), the background material becomes a medium of higher index and behaves like a defect in an otherwise lower-index material. This is in opposite to the normal air-defect state, where the air has a lower index.

C. Physical mechanism of resonant cavitylike modes

The appearance of collective modes in the present problem is closely related to the artificial magnetism that arises in the high-dielectric subwavelength cylinders. A large dielectric contrast $(\varepsilon_1/\varepsilon)$ between the cylinder and surrounding material is crucial for giving rise to strong magnetism. This phenomenon is attributed to the existence of large polarization currents circulating around the dielectric cylinders, which give rise to a substantial magnetic dipole moment along the cylinder axis.[3] In this situation, the electromagnetic fields tend to localize within the high-dielectric region. This feature is particularly true for the magnetic fields; they are required only to be continuous (rather than both continuous and smooth as for the electric fields) at the interface between two different media. Similar phenomena have also been reported in the dielectric metamaterials.[20,21]

According to the effective medium model, Eq. (7), for the dielectric structure, the effective permeability can grow to a very large value as the resonant condition is approached. The building block of the structure in Fig. 1 has in effect a very large index of refraction. In this situation, the electromagnetic fields are almost trapped inside the cylinders and the building block behaves like a waveguide or cavity resonator. As the building blocks are arranged to form a periodic lattice, a large number of collective modes appear and gather around a particular frequency. The underlying mechanism is attributed to the coupling of Mie resonance (due to individual cylinders) with the Bragg resonance (due to periodicity of the lattice). As these modes share some common features with the resonant cavity modes that appear in polaritonic crystals,[8] they are termed as resonant cavitylike modes in this study.

The geometry of the photonic structure, including the shapes of building block and subwavelength cylinder, has a minor effect on the basic features of resonant cavitylike

modes. These collective modes may appear in other geometries as well, as long as the subwavelength cylinders possess a large dielectric contrast and the collection of cylinders behave like an effective medium so that the effective permeability model is applicable. The effect of geometry, however, is the shift of resonant frequency with respect to the cylinder size, as has been illustrated in Fig. 3.

IV. CONCLUDING REMARKS

In conclusion, we have investigated resonant cavitylike modes in dielectric photonic crystals made of collections of subwavelength cylinders. The underlying photonic structure behaves like a magnetic analog of polaritonic crystal, where the subwavelength cylinders serve as a mechanism for trapping electromagnetic fields. Existence of resonant cavitylike modes is manifest on the collective frequency branches and localized field patterns. At the resonant frequencies, the building block acts like an isolated waveguide with regard to the mode pattern and cutoff frequency. As the properties of resonant cavitylike modes can be engineered by the subwavelength cylinders, the underlying photonic structures are eligible to be polaritonic metamaterials.

ACKNOWLEDGMENTS

This work was supported in part by the National Science Council of the Republic of China under Contracts No. NSC 96-2221-E-002-190-MY3 and No. 98-2120-M-002-004, and by the French National Research Agency under Grant No. ANR PNANO-06-NANO-008 POEM.

APPENDIX

The effective permittivity ε_{eff} of the dielectric structure [Eq. (15)] can be determined by requiring that the total polarizability of a unit cell of the microstructure, when embedded in an effectively homogeneous medium, be zero. Figure 6 shows a schematic of the unit cell, consisting of a square dielectric cylinder (with permittivity ε_1) and the surrounding material (with permittivity ε), placed in the effective medium (with the permittivity ε_{eff}). Let α_1 and α be the polarizabilities (per unit length) attributed to the dielectric cylinder and the unit cell, respectively. The condition of the effective medium to be valid is given by $\alpha_1+\alpha=0$. When this condition holds, the respective unit cell is indistinguishable with respect to the effective medium from the polarization point of view. The unit cell has therefore the same permittivity as the effective medium. Similar approaches based on zero scattering fields of the unit cell have been applied to the effective parameters for circular cylinders and spheres in an analytical manner.[22–24]

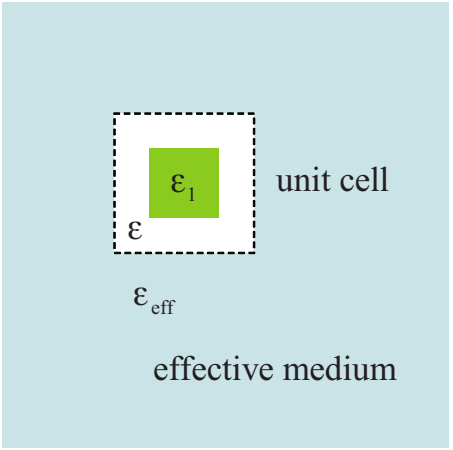

FIG. 6. (Color online) Schematic of a unit cell of the microstructure (denoted by the dashed line) embedded in an effective medium.

For square cylinders, the polarizability has no analytical form but can be characterized by an approximate model as[19]

$$\alpha_1 \approx \varepsilon_0 A_1 \frac{2.18(\varepsilon_1-\varepsilon)}{\varepsilon_1-1.29\varepsilon}, \quad \alpha \approx \varepsilon_0 A \frac{2.18(\varepsilon_{\text{eff}}-\varepsilon)}{\varepsilon_{\text{eff}}-1.29\varepsilon}, \tag{A1}$$

where A_1 and A are the areas of the cylinder and the unit cell, respectively, and therefore $f=A_1/A$. Using Eq. (A1) in $\alpha_1+\alpha=0$, ε_{eff} is solved to give

$$\varepsilon_{\text{eff}} \approx \varepsilon \frac{(1+1.29f)\varepsilon_1+1.29(1-f)\varepsilon}{(1-f)\varepsilon_1+(1.29+f)\varepsilon}. \tag{A2}$$

It is noted that for circular cylinders the polarizability is given as[19]

$$\alpha_1 = 2\varepsilon_0 A_1 \frac{\varepsilon_1-\varepsilon}{\varepsilon_1-\varepsilon}, \quad \alpha = 2\varepsilon_0 A \frac{\varepsilon_{\text{eff}}-\varepsilon}{\varepsilon_{\text{eff}}-\varepsilon}. \tag{A3}$$

The above relations yield

$$\varepsilon_{\text{eff}} = \varepsilon \frac{(1+f)\varepsilon_1+(1-f)\varepsilon}{(1-f)\varepsilon_1+(1+f)\varepsilon}, \tag{A4}$$

which is the two-dimensional version of the well-known Maxwell-Garnett mixing rule.[25] A comparison between Eqs. (A2) and (A3) shows that there is a slight discrepancy of ε_{eff} between the square and circular cylinders.

*chern@iam.ntu.edu.tw

[1] J. B. Pendry, A. J. Holden, D. J. Robbins, and W. J. Stewart, IEEE Trans. Microwave Theory Tech. **47**, 2075 (1999).
[2] D. R. Smith, J. B. Pendry, and M. C. K. Wiltshire, Science **305**, 788 (2004).
[3] S. O'Brien and J. B. Pendry, J. Phys.: Condens. Matter **14**, 4035 (2002).
[4] D. Felbacq and G. Bouchitté, Phys. Rev. Lett. **94**, 183902 (2005).
[5] K. C. Huang, P. Bienstman, J. D. Joannopoulos, K. A. Nelson,

and S. Fan, Phys. Rev. Lett. **90**, 196402 (2003).
[6] K. C. Huang, P. Bienstman, J. D. Joannopoulos, K. A. Nelson, and S. Fan, Phys. Rev. B **68**, 075209 (2003).
[7] G. Gantzounis and N. Stefanou, Phys. Rev. B **72**, 075107 (2005).
[8] R. L. Chern, C. C. Chang, and C. C. Chang, Phys. Rev. B **73**, 235123 (2006).
[9] G. Gantzounis and N. Stefanou, Phys. Rev. B **75**, 193102 (2007).
[10] D. Felbacq and G. Bouchitté, Opt. Lett. **30**, 1189 (2005).
[11] D. Felbacq and G. Bouchitté, New J. Phys. **7**, 159 (2005).
[12] R. L. Chern and D. Felbacq, Phys. Rev. B **79**, 075118 (2009).
[13] N. A. Mortensen, S. Xiao, and D. Felbacq, J. Eur. Opt. Soc. Rapid Publ. **1**, 06019 (2006).
[14] D. M. Pozar, *Microwave Engineering*, 3rd ed. (Wiley, New York, 2005).
[15] C. Kittel, *Introduction to Solid State Physics*, 8th ed. (Wiley, New York, 2005).
[16] R. L. Chern, C. C. Chang, C. C. Chang, and R. R. Hwang, Phys. Rev. E **68**, 026704 (2003).
[17] C. C. Chang, J. Y. Chi, R. L. Chern, C. C. Chang, C. H. Lin, and C. O. Chang, Phys. Rev. B **70**, 075108 (2004).
[18] R. L. Chern and S. D. Chao, Opt. Express **20186**, 16600 (2008).
[19] J. Avelin, R. Sharma, I. Hanninen, and A. H. Sihvola, IEEE Trans. Antennas Propag. **49**, 451 (2001).
[20] J. A. Schuller, R. Zia, T. Taubner, and M. L. Brongersma, Phys. Rev. Lett. **99**, 107401 (2007).
[21] L. Peng, L. Ran, H. Chen, H. Zhang, J. A. Kong, and T. M. Grzegorczyk, Phys. Rev. Lett. **98**, 157403 (2007).
[22] Y. Wu, J. Li, Z. Q. Zhang, and C. T. Chan, Phys. Rev. B **74**, 085111 (2006).
[23] X. Hu, C. T. Chan, J. Zi, M. Li, and K. M. Ho, Phys. Rev. Lett. **96**, 223901 (2006).
[24] S. T. Chui and Z. Lin, Phys. Rev. E **78**, 065601(R) (2008).
[25] J. C. Maxwell-Garnett, Philos. Trans. R. Soc. London, Ser. A **203**, 385 (1904).